Lymphology 58 (2025) 159-164

SPATIAL RELATIONSHIPS OF THE CISTERNA CHYLI AND ABDOMINAL VENOUS VASCULATURE ON MRI

M. Cutlan, E. M. Knavel Koepsel, G. V. Toia, E. J. Monroe

University of Wisconsin School of Medicine and Public Health, USA (MC); University of Wisconsin School of Medicine and Public Health Department of Radiology, USA (EMKK,GVT,EJM); University of Wisconsin School of Medicine and Public Health Department of Medical Physics, USA (GVT).

ABSTRACT

In the field of interventional radiology, transvascular routes of access to adjacent structures have led to shorter procedure times and fewer complications. No transvenous approach to intervene on the lymphatic ducts currently exists, nor do any standard measurements of the inferior vena cava (IVC) and cisterna chyli (CC). This retrospective review of cross-sectional imaging studies consisted of 150 adults (age 57±17.8) who obtained a magnetic resonance pancreatography (MRCP) for a variety of clinical indications. Of those, 8 patients had poor image quality and 28 did not have an identifiable CC. The remaining 114 images were evaluated for size, caliber, and orientation of anatomic structures of interest using a PACS workstation. The average distance between the center of the IVC to the center of the CC was found to be 24.3 mm (11.1-50.5 mm). The angle relative to anterior-posterior as determined by the spine ranged from 21.0° anterior to 103.0° posterior. Important intervening structures included the renal artery (19.30%), liver (7.02%), and aorta (4.39%). The short spatial approximation of the IVC and CC and the rarity of intervening structures support further development of transvascular CC access techniques.

Keywords: Cisterna chyli; Inferior vena cava; Magnetic resonance pancreatography; Anatomy; Imaging

INTRODUCTION

The cisterna chyli (CC) is a retroperitoneal lymphatic structure that collects lymph from the abdominopelvic viscera and lower extremities and drains into the thoracic duct. Although the role of the CC is well described, there is anatomic variation in the CC in terms of location, size, morphology, and tributaries. The CC has been visually documented on a variety of imaging techniques such as computed tomography (CT) and lymphangiography (1,2). Ultimately, magnetic resonance imaging (MRI) has demonstrated a higher incidence of detecting the CC compared to CT or lymphangiography (3,4).

A spectrum of lymphatic disorders exist and involve problems with either lymph drainage or lymphatic congestion. Examples include chylothorax, plastic bronchitis, chylous ascites, idiopathic chyluria, lymphocele, and lymphorrhea. These lymphatic disorders can be managed via lymphatic interventional techniques, including thoracic duct embolization, interstitial lymphatic embolization, liver lymphatic embolization, thoracic duct lymphoplasty and stenting, and retrograde thoracic duct access.

(5). Despite anatomic variation, the CC remains an important structure to identify for access to central lymphatics and other interventional radiology techniques.

One lymphatic disorder to further explore is chylothorax. The thoracic duct is at risk of injury during various thoracic procedures, such as esophagectomy and lung resection due to its anatomical position. Chylothorax, the resulting injury, occurs at an incidence ranging from 1-9% and poses a significant risk of morbidity and mortality if not managed effectively (6). Invasive management strategies typically involve accessing the CC transabdominally with a needle, followed by catheterization and embolization of the thoracic duct or abdominal and retroperitoneal ducts. This access technique may be complicated by patient habitus and/or respiratory motion, and the route of access inherently poses risks of complications stemming from the transvisceral passage of equipment (7). Prior work has demonstrated that such transvisceral access commonly involves structures including the liver, pancreas, and vascular structures, yet is generally well tolerated with a low rate of clinically significant complications (8). Upon failed transabdominal CC cannulation, percutaneous fluoroscopically-guided transcervical retrograde thoracic duct access and embolization have been shown to be a safe and technically successful alternate method (9).

In interventional radiology, transvascular routes of access to adjacent structures have led to shorter procedure times and fewer complications in procedures, such as transjugular intrahepatic portosystemic shunt creation (10,11). This advancement has been aided by the development of intravascular ultrasound (IVUS) (10,11). No transvenous approach to intervene on the lymphatic ducts currently exists, nor do any standard measurements of the relationship between the inferior vena cava (IVC) and CC to each other. The approximation of the IVC and CC affords an opportunity for a novel transvascular approach to central lymphatic access and intervention. The purpose of this study was to detail the anatomic relationship between the IVC and CC on MRI. The hypothesis is that the CC lies in close spatial proximity to the IVC such that it is within the imaging field of currently available IVUS systems, and that intervening structures, though potentially present, are infrequent and would be identifiable with IVUS.

MATERIALS AND METHODS

Patient Population

This Health Insurance Portability and Accountability Act compliant retrospective study was conducted at a single academic university hospital and approved by the University of Wisconsin School of Medicine and Public Health Institutional Review Board. Informed consent requirements were waived given the retrospective nature of this work. All MRCP scans obtained during a two-month period (1/1/2024-2/29/2024) were identified via electronic medical record systems. The study population was 150 patients who received MRCP for a variety of clinical indications. Patients were all 18 years of age or older.

MRI Techniques

All scans were performed in accordance with institutional MRCP protocols on a variety of 1.5T (SIGNA Artist, Optima MR450w, SIGNA HDxt) and 3.0T (Discover MR750, SIGNA Architect, SIGNA Premier) magnets from a single vendor (GE Healthcare, Waukesha, WI). After a 6-hour fasting period, patients underwent 2D axial and coronal (T2w Steady State Fast Spin Echo) and 3D coronal MRCP using respiratory triggering. Settings for 1.5T scanners were TR = 1000-3818 ms, TE = 248-251 ms, Flip Angle = 90°, and Number of Excitations = 0.70-.99, slice thickness = 3 mm (2D) / 1.8 mm (3D) without slice gap, matrix = 320 x 224 (2D) / 288 x 288 (3D), and field of view = 300 x 80 mm (2D) / 350 x 100 mm (3D). Settings for 3.0T scanners were TR = 1400-4667 ms, TE = 247-252 ms, Flip Angle = 90-130°, Number of Excitations = 0.80-.99, slice thickness = 3mm (2D) / 1.8 mm (3D) without slice gap, matrix = 384 x 256 (2D) / 288 x 288 (3D), and field of view = 320 x

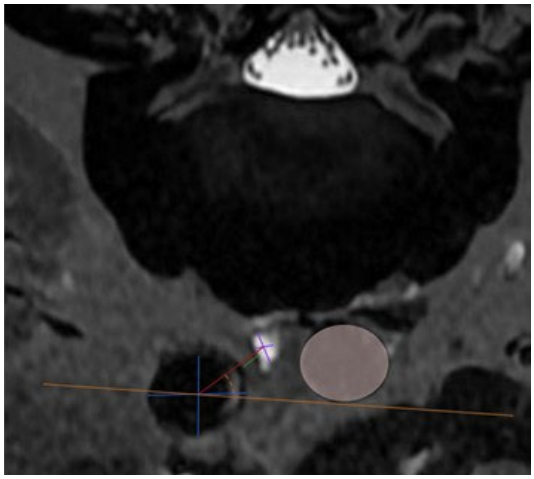

Fig. 1. *Example imaging measurements of the CC on 2D axial MRCP. The major and minor axes of the IVC (blue lines) and CC (purple lines) were noted. The distance between the center of the IVC and the center of the CC (red line) and the distance between the wall of the IVC and wall of the CC (green line) were measured. The angle relative to anterior-posterior as determined by the spine (dashed orange line) was recorded. Lastly, the position of the CC relative to the aorta (shaded in pink) was noted as either right-sided or left-sided. (MRCP = magnetic resonance cholangiopancreatography).*

100 mm (2D) / 340 x 90 mm (3D). Additional pulse sequences per institutional protocol were also obtained but excluded from analysis: axial T1w pre and post contrast with fat saturation, axial T2w fat with fat saturation, axial diffusion weighting imaging, and coronal T1w post contrast delayed images.

Image Interpretation

All 2D axial and coronal images were evaluated on a PACS workstation and independently interpreted by a medical student with imaging training and an experienced, fellowship-trained abdominal radiologist. Discrepancies between the readers were discussed and resolved by consensus. The images were first screened for proper image quality and the presence of a CC. Image quality was assessed by motion artifacts noted on scans and spatial resolution. The CC was identified as a fluid collection with a diameter of 2.5 mm or more and a signal intensity similar to that of cerebrospinal fluid in the retrocrural space. Images were evaluated for 1) shape, dimensions, and location of the CC; 2) dimensions and location of the IVC; 3) intervening structures between the CC and the IVC; and 4) relationship between the CC and the IVC (*Fig. 1*). The CC was identified by the presence of a fluid-filled structure in the retrocrural space.

RESULTS

The study population consisted of a total of 150 patients, 66 male (44%) and 84 female (56%), average age 57±17.8. Out of the initial 150 patients, 8 patients had poor image quality (due to motion artifact or poor spatial resolution, resulting in non-diagnostic quality images) and 28 patients did not have an identifiable CC. Once these patients were excluded, the remaining 114 patients' images were evaluated.

The majority of cases featured a CC on the right side of the aorta (*Fig. 2*). However, 5 cases were found to be left-sided (*Fig. 3*). The average distance between the center of the IVC to the center of the CC was found to be 24.3 mm (11.1-50.5 mm). The average distance between the wall of the IVC and the wall of the CC was found to be 14.1 mm (3.42-41.8 mm). The angle relative to anterior-posterior as determined by the spine ranged from 21.0° anterior to 103.0° posterior (*Fig. 4*). Although the majority of CCs were located posteromedially from the IVC (81.6%), 17.54% of CCs were located anteromedially to the IVC.

Several intervening structures between the IVC and the CC were noted (*Table 1*). "Close but not intervening" was defined as a structure visualized within the same anatomic plane and in near proximity to the IVC–CC axis, but not crossing or occupying the direct line of potential access between them. Important intervening structures noted included the renal artery (19.30%), liver (7.02%), aorta (4.39%), right phrenic artery (0.88%), and stomach (0.88%).

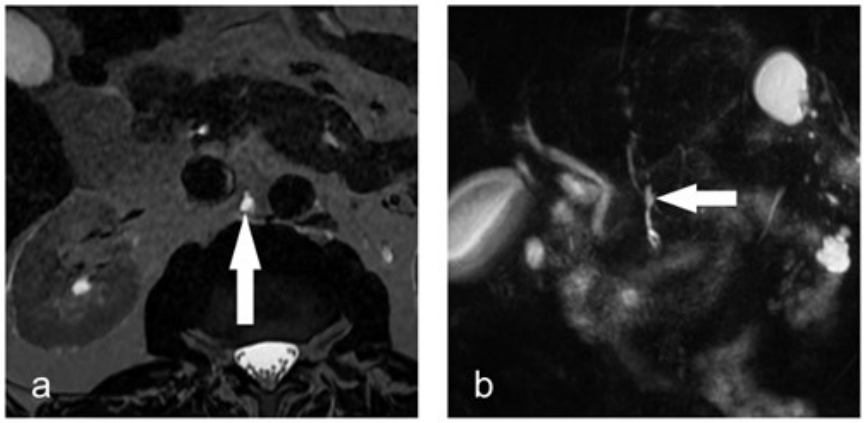

Fig. 2. *Normal CC in a 65-year-old male with BRCA2 cancer predisposition undergoing MRCP for surveillance. Axial 2D (1.5T, TR 2210.52 ms, TE 250.9 ms) MR image (a) and coronal 3D MIP (1.5T, TR 6666.67 ms, TE 700.6 ms) MR image (b) demonstrate a normal CC (arrows).*

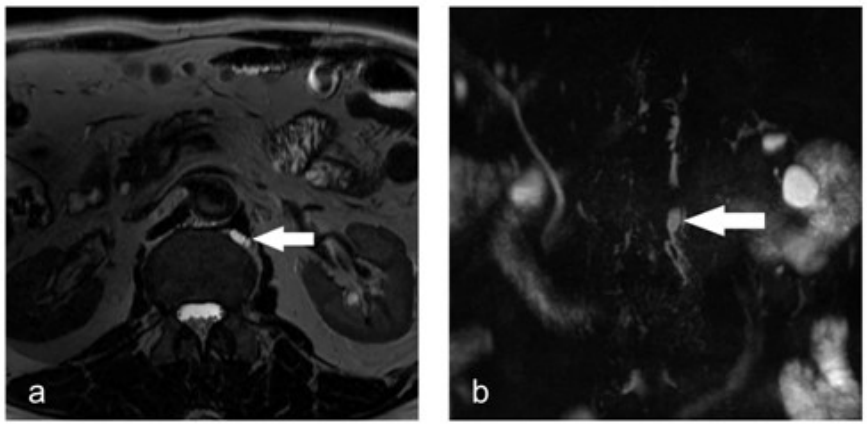

Fig. 3. *Left-sided CC in a 69-year-old male patient undergoing MRCP for pancreatic cyst follow-up. Axial 2D (3T, TR 2210.52 ms, TE 250.9 ms) MR image (a) and coronal 3D MIP (3T, TR 3157.90 ms, TE 579.0 ms) MR image (b) demonstrate a left-sided CC (arrows).*

DISCUSSION

The CC was localized and measured in 76% of patient MRI MRCPs. From these 114 patients, the anatomic relationship between the IVC and CC was characterized, including the distance, angle, and intervening structures. This work serves as a foundational anatomic exploration, establishing spatial relationships that may inform future procedural innovation.

Building on these findings, the observed proximity and orientation of the CC relative to the IVC suggest a potential framework for further investigation. Given the established utility of IVUS in interventional radiology, it is reasonable to hypothesize that IVUS within the IVC could allow for visualization of the CC. The average distance between the wall of the IVC and the wall of the CC described here falls within the field of view of currently available side-firing IVUS catheters, which typically have a maximum display depth of 14-21 cm depending on the device type (10). While intervening structures were identified in some cases, they were not predominant and would likewise be expected to be detectable with

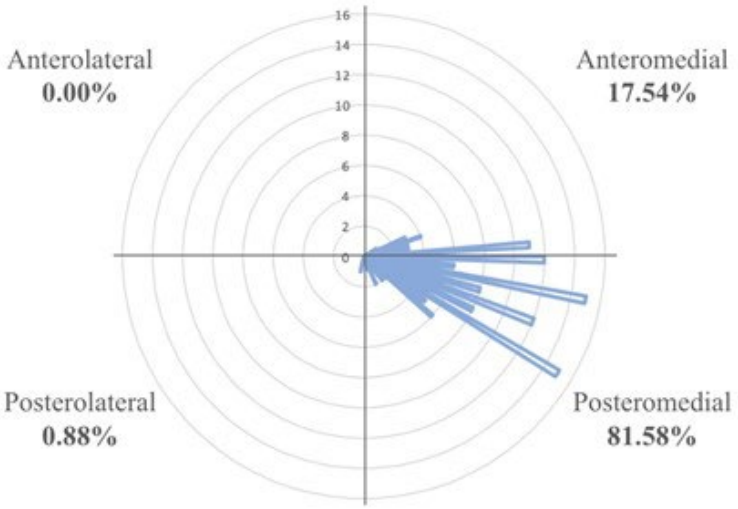

Fig. 4. *Radial histogram representing the distribution of angles at which the CC is located relative to the IVC.*

TABLE 1
Intervening Structures Identified by Imaging Between the IVC and CC

STRUCTURE	Number of Patients	Percent of Patients
Renal Artery	22	19.3
Renal Artery close but not intervening	7	6.1
Liver	8	7.0
Liver close but not intervening	6	5.3
Aorta	5	4.4
Right phrenic artery	1	0.9
Adrenal gland close but not intervening	2	1.8
Gastric veins/stomach (hiatal hernia)	1	0.9

IVUS imaging. Such an approach may support the conceptual development of image-guided, transvascular access to the CC. While this remains theoretical, it offers a possible pathway to reduce reliance on conventional lymphangiography, which is associated with higher radiation exposure, contrast use, and the risks inherent to transvisceral access (10).

CONFLICT OF INTEREST

All authors declare no competing financial interests exist.

REFERENCES

1. Smith, TR, J Grigoropoulos: The cisterna chyli: Incidence and characteristics on CT. Clin. Imaging. 26 (2002), 18–22.
2. Rosenberger, A, JL Abrams: Radiology of the thoracic duct. Amer. J. Roentgenol. Ra. 111 (1971), 807–820.
3. Katsuyoshi, I, A Shimizu, M Tanabe, et al: Cisterna chyli in patients with portal hypertension: Evaluation with MR imaging. J. Magn. Reson. Imaging 35 (2012), 624-628.
4. Pinto, PS, CB Sirlin, OA Andrade-Barreto, et al: Cisterna chyli at routine abdominal MR

imaging: A normal anatomic structure in the retrocrural space. Radiographics. 24 (2004), 809–817.
5. Benjamin, J, C O'Leary, S Hur, et al: Imaging and interventions for lymphatic and lymphatic-related disorders. Radiology. 307 (2023), e220231.
6. Jun, H, S Hur: Interventional radiology treatment for postoperative chylothorax. Korean J. Thorac. Cardiovasc. Surg. 53 (2020), 200-204.
7. Chen, E, M Itkin: Thoracic duct embolization for chylous leaks. Semin. Intervent. Radiol. 28 (2011), 63-74.
8. Schild, HH, Pieper, CC: Where have all the punctures gone? An analysis of thoracic duct embolizations. J. Vasc. Interv. Radiol. 31 (2020), 74-79.
9. Bundy, JJ, CA Jiao, MR Cline, et al: Percutaneous fluoroscopically-guided transcervical retrograde access facilitates successful thoracic duct embolization after failed antegrade transabdominal access. Lymphology. 52 (2019), 52-60.
10. Woods, MA, EM Knavel Koepsel, JF Swietlik, et al: Intravascular US: Applications in interventional radiology. RadioGraphics. 42 (2022), 1742-1757.
11. Weaver, JJ, DS Shin, JFB Chick, et al: Intravascular ultrasound for endovascular precision in pediatrics. Pediatr. Radiol. 52 (2022), 559-569.

Eric J Monroe, MD
University of Wisconsin School of Medicine and Public Health
Department of Radiology
E-mail: EMonroe@uwhealth.org